

Dynamical Simulations of Polaron Transport in Conjugated Polymers with the Inclusion of Electron–Electron Interactions

Haibo Ma* and Ulrich Schollwöck†

Institute for Theoretical Physics C, RWTH Aachen University, D-52056 Aachen, Germany

Received: October 13, 2008; Revised Manuscript Received: October 31, 2008

Dynamical simulations of polaron transport in conjugated polymers in the presence of an external time-dependent electric field have been performed within a combined extended Hubbard model (EHM) and Su–Schrieffer–Heeger (SSH) model. Nearly all relevant electron–phonon and electron–electron interactions are fully taken into account by solving the time-dependent Schrödinger equation for the π electrons and the Newton’s equation of motion for the backbone monomer displacements by virtue of the combination of the adaptive time-dependent density matrix renormalization group (TDDMRG) and classical molecular dynamics (MD). We find that after a smooth turn-on of the external electric field, the polaron is accelerated at first and then moves with a nearly constant velocity as one entity consisting of both the charge and the lattice deformation. An ohmic region ($3 \leq E_0 \leq 9$ mV/Å) where the stationary velocity increases linearly with the electric field strength is observed for the case of $U = 2.0$ eV and $V = 1.0$ eV. The maximal velocity is well above the speed of sound. Below 3 mV/Å, the polaron velocity increases nonlinearly, and in high electric fields with strengths of $E_0 \geq 10.0$ mV/Å, the polaron will become unstable and dissociate. The relationship between electron–electron interaction strengths and polaron transport is also studied in detail. We find that the on-site Coulomb interactions U will suppress the polaron transport, and small nearest-neighbor interactions V values are also not beneficial to the polaronic motion while large V values favor the polaron transport.

I. Introduction

Charge-transport properties in conjugated polymers have attracted sustained attention from both academic and industrial researchers since it was discovered in the 1970s that the electrical conductivity of *trans*-polyacetylene (PA) can be improved significantly by doping with strong electron acceptors or donors.^{1–3} Many electronic devices have been fabricated based on these conjugated polymers.^{4–7}

All of the conducting polymers can generally be sorted into two classes. The first class is *trans*-polyacetylene, in which there exists a two-fold degeneracy of ground-state energy distinguished by the positions of the double and single bonds. The degenerate ground state of *trans*-polyacetylene leads to solitons⁸ as the important excitations and the dominant charge storage species, which take the form of domain walls separating different districts of opposite single- and double-bond alternation patterns. The second class of conducting polymers is given by all of the other systems except *trans*-polyacetylene, in which the ground-state degeneracy is weakly lifted. Therefore, polarons and confined soliton pairs (bipolarons)⁸ instead of solitons are the important excitations and the dominant charge storage configurations for this class of conducting polymers. Nowadays, it has been widely accepted that these quasiparticles (solitons, polarons, and bipolarons) are the fundamental charge carriers in conducting polymers. The studies of the dynamics of these charge carriers are therefore of great interest for the purpose of modulating or devising new organic electronic materials based on conjugated polymers.

So far, there have been many extensive theoretical studies on polaron dynamics in conjugated polymers^{9–20} based on the

Su–Schrieffer–Heeger (SSH) model,^{21,22} an improved Hückel molecular orbital model, in which π electrons are coupled to distortions in the polymer backbone by the electron–phonon interaction. Rakhmanova and Conwell^{9,10} have considered the motion of a polaron under low and high electric fields, respectively, by using an adiabatic simulation in which the electronic energy is treated within the Born–Oppenheimer approximation. Their results show that the polaron can form and move in its entity in low electric fields but dissociates in high fields. The highest electric field strength under which the polaron can sustain is about 6 mV/Å. Basko and Conwell¹¹ have also analyzed the dynamics of a polaron and found that the speed of a steadily moving polaron cannot exceed the sound speed (V_S). These conclusions are consistent with those from the numerical results presented by Arikabe et al.¹² but inconsistent with those given by Johansson and Stafström,^{13,14} who performed a nonadiabatic simulation in which transitions between instantaneous eigenstates were allowed. In Johansson and Stafström’s work, the maximum velocity (about $4 V_S$) is reached at a high electric field strength (~ 3.5 mV/Å), and at even higher electric field strengths, the polaron will become unstable and dissociate.

In the SSH model, only the electron–lattice interactions are considered, and the electron–electron interactions are totally ignored. In order to improve this situation, Di et al. have considered the extended Hubbard model (EHM) combined with the SSH model and investigated the dynamics of polarons within this model at the level of an unrestricted Hartree–Fock (UHF) approximation.²³ They found that the localization of the polaron is enhanced and the stationary velocity of the polaron is decreased by both the on-site repulsions U and the nearest-neighbor interactions V . Furthermore, they found that the local extremum of the stationary velocity of the polaron appears at $U \approx 2V$. However, in recent years, a lot of theoretical

* To whom correspondence should be addressed. E-mail: haiboma@physik.rwth-aachen.de.

† E-mail: scholl@physik.rwth-aachen.de.

calculations of the static properties of conjugated polymers have shown that the electron correlation effect plays a very important role in determining the behavior of the charge carriers in conjugated polymers.^{24–40} For example, electron correlation is essential in obtaining correct pictures of the spin polarizations in *trans*-polyacetylene.³⁸ Therefore, theoretical simulations for polaron dynamics with electron correlations considered, which step beyond the SCF level, are highly desirable. Due to the exponential growth of the number of degrees of freedom in quantum many-body systems, the exact simulation in the complete Hilbert space is apparently not feasible beyond very small sizes. A great number of various approximate simulation methods for quantum many-body systems attempt a systematic choice of a subspace of the complete Hilbert space which is anticipated to contain the physically most relevant states. Among them, the density matrix renormalization group (DMRG) method proposed by White in 1992,^{41,42} which uses the eigenvalues of the subsystem's reduced density matrix as the decimation criterion, has been shown as an extremely accurate technique in solving one-dimensional strongly correlated systems with economic computational costs.⁴³ In recent years, a time evolution scheme for DMRG, the adaptive time-dependent density matrix renormalization group (TDDMRG) method^{43–45} which evolves the correlated quantum system within adaptive truncated Hilbert spaces, has been developed and provides us with an efficient way to accurate dynamical simulations with electron correlation effects taken into account. In the context of 1D correlated electronic and bosonic systems, the adaptive TDDMRG has been found to be a highly reliable real-time simulation method at economic computational cost, for example, in the context of magnetization dynamics,⁴⁶ spin–charge separation,^{47,48} or far-from equilibrium dynamics of ultracold bosonic atoms.⁴⁹ Recently, Zhao et al. have performed adaptive TDDMRG simulations for polaronic transport within a combined model of SSH and the Hubbard model to take the on-site Coulomb interactions into account and found that that the velocity of the polaron is suppressed by the on-site Coulomb interaction U .⁵⁰

In this paper, combining the SSH and extended Hubbard model to take both the on-site Coulomb interactions and nearest-neighbor electron–electron interactions into account, we simulate the motion of a polaron in conjugated polymers under an applied external electric field by using the adaptive TDDMRG for the π electron part and classical molecular dynamics (MD) for the lattice backbone part. The aim of this paper is to give an exhaustive picture of polaron transport in conducting polymers at a theoretical level with all relevant electron–electron interactions and correlations included and to show how the on-site Coulomb interactions U and nearest-neighbor electron–electron interactions V influence the behavior of polaron transport in conducting polymers.

II. Model and Methodology

We use the well-known and widely used SSH Hamiltonian^{21,22} combined with the extended Hubbard model (EHM) and include the external electric field by an additional term

$$H(t) = H_{\text{el}} + H_{E(t)} + H_{\text{lat}} \quad (1)$$

This Hamiltonian is time-dependent because the electric field $E(t)$ is explicitly time-dependent.

The π electron part includes both the electron–phonon and the electron–electron interactions

$$H_{\text{el}} = - \sum_{n,\sigma} t_{n,n+1} (c_{n+1,\sigma}^+ c_{n,\sigma} + \text{h.c.}) + \frac{U}{2} \sum_{n,\sigma} (c_{n,\sigma}^+ c_{n,\sigma} - \frac{1}{2}) (c_{n,-\sigma}^+ c_{n,-\sigma} - \frac{1}{2}) + V \sum_{n,\sigma,\sigma'} (c_{n,\sigma}^+ c_{n,\sigma} - \frac{1}{2}) (c_{n+1,\sigma'}^+ c_{n+1,\sigma'} - \frac{1}{2}) \quad (2)$$

where $t_{n,n+1}$ is the hopping integral between the n th site and the $(n+1)$ th site, while U is the on-site Coulomb interaction, and V denotes the nearest-neighbor electron–electron interaction. Because the distortions of the lattice backbone are always within a certain limited extent, one can adopt a linear relationship between the hopping integral and the lattice displacements as $t_{n,n+1} = t_0 - \alpha(u_{n+1} - u_n)$,^{21,22} where t_0 is the hopping integral for zero displacement, u_n the lattice displacement of the n th site, and α the electron–phonon coupling.

Because the atoms move much slower than the electrons, we treat the lattice backbone classically with the Hamiltonian

$$H_{\text{lat}} = \frac{K}{2} \sum_n (u_{n+1} - u_n)^2 + \frac{M}{2} \sum_n \dot{u}_n^2 \quad (3)$$

where K is the elastic constant and M is the mass of a site, such as that of a CH monomer for *trans*-polyacetylene.

The electric field $E(t)$ directed along the backbone chain is uniform over the entire system. The field which is constant after a smooth turn-on is chosen to be

$$E(t) = \begin{cases} E_0 \exp[-(t - T_C)^2/T_W^2] & \text{for } t < T_C \\ E_0 & \text{for } t \geq T_C \end{cases} \quad (4)$$

where T_C , T_W , and E_0 are the center, width, and strength of the half Gaussian pulse. This field gives the following contribution to the Hamiltonian

$$H_{E(t)} = |e| \sum_{n,\sigma} (na + u_n) (c_{n,\sigma}^+ c_{n,\sigma} - \frac{1}{2}) E(t) \quad (5)$$

where e is the electron charge and a is the unit distance constant of the lattice. The model parameters are those generally chosen for polyacetylene, $t_0 = 2.5$ eV, $\alpha = 4.1$ eV/Å, $K = 21$ eV/Å², $M = 1349.14$ eV fs²/Å², $a = 1.22$ Å.²² The results are expected to be qualitatively valid for the other conjugated polymers. The values of T_C and T_W ($T_C = 30$ fs and $T_W = 25$ fs) are taken from the paper of Fu et al.¹⁸

For the purpose of performing real-time simulation of both the evolution of the quantum π electron part and the classical movement of the chain backbone, we adopt a newly developed real-time simulation method in which classical molecular dynamics is combined with the adaptive TDDMRG. The main idea of this method is to evolve the π electron part by the adaptive TDDMRG and move the backbone part by classical MD iteratively. Details about this method can be found in recent papers.^{50,51} We have carefully studied the accuracy performance of the combined TDDMRG/MD method. Normally, in the analysis of reduced-density matrices, the advantage of DMRG is that the weight of the states in the reduced density matrix that are then discarded (“truncation weight”) is a highly efficient control parameter for the accuracy of the method. We found that one can get reliable and converged numerical results if the DMRG truncation weight ϵ_ρ is taken small enough ($\epsilon_\rho \leq 1.0 \times 10^{-6}$), and suitable time step Δt values around 0.01–0.05 fs are chosen.⁵¹ In the recent work by Zhao et al., the excellent agreement of TDDMRG/MD results with the exact numerical results for a noninteracting chain ($U = 0$, $V = 0$) also verified the reliability of the combined TDDMRG/MD method.⁵⁰ All

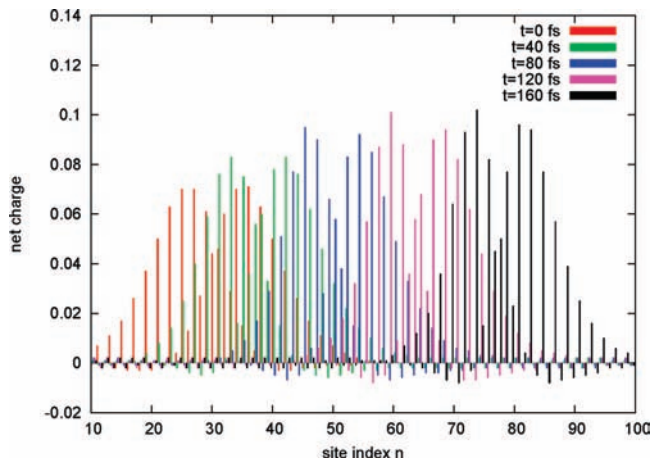


Figure 1. Time evolution of the net charge distribution in a polymer chain with the transport of a polaron under an external electric field (the polaron moves from the left to the right) ($E_0 = 3.0$ mV/Å, $U = 2.0$ eV, $V = 1.0$ eV).

of our numerical results presented in this work are well-converged values calculated with $\epsilon_\rho = 5.0 \times 10^{-7}$ and $\Delta t = 0.05$ fs.

III. Results and Discussion

To investigate the dynamic properties of polarons, we simulate the polaron-transport process in a single-model conjugated polymer chain under a uniform external electric field. A polaron is different from a charged soliton in that it involves an unpaired electron and thus a nonzero $S = 1/2$. In our calculations, we simulate a model chain containing $N = 100$ monomers and $N_e = 99\pi$ electrons to present a polaron defect without degenerate ground states. The polaron is initially centered around sites 30 and 31 through imposing a constraint of reflection symmetry around the center between sites 30 and 31. Then, the dynamics of polaron transport in 160 fs is simulated by virtue of classical MD combined with the adaptive TDDMRG.

A. General Picture of Polaron Transport. First let us show the general time evolution picture of polaron transport in a conducting polymer. The time evolution of charge density and the staggered bond order parameter $r_n = (-1)^n(2u_n - u_{n+1} - u_{n-1})/4$ in a polymer chain with a polaron defect are shown in Figures 1 and 2. It can be clearly seen that both the charge density and the geometrical distortions do not localize at one monomer. On the contrary, the polaron defect spreads over a delocalized region with a length of tens of sites. One can also clearly see that during the entire time evolution process, the geometrical distortion curve and net charge distribution shape for the polaron defect always stay coupled and show no obvious dispersion. This implies that the polaron defect is an inherent feature and the fundamental charge carrier in conducting polymers. In Figure 2, we can also see that a long-lasting oscillatory “tail” appears behind the polaron defect center. This “tail” is generated by the inertia of those monomers to fulfill energy and momentum conservation; they absorb the additional energy, preventing the further increase of the polaron velocity after a stationary value is reached.

In order to evaluate the velocity of polaron transport, it is necessary to know the center positions of a polaron at different times. The center position of a defect can be derived from the charge density distribution picture or the bond length alternation pattern as

$$x_{c,g}(t) = \begin{cases} N\theta_{c,g}(t)/2\pi & \text{if } \cos \theta_{c,g} \geq 0 \text{ and } \sin \theta_{c,g} \geq 0 \\ N(\pi + \theta_{c,g}(t))/2\pi & \text{if } \cos \theta_{c,g} < 0 \\ N(2\pi + \theta_{c,g}(t))/2\pi & \text{otherwise} \end{cases} \quad (6)$$

where $\theta_{c,g}$ is defined according to the charge density ρ_n or the staggered bond order parameter r_n as

$$\theta_c(t) = \arctan \frac{\sum_n \rho_n(t) \sin(2\pi n/N)}{\sum_n \rho_n(t) \cos(2\pi n/N)} \quad (7)$$

$$\theta_g(t) = \arctan \frac{\sum_n (r_n(t) - r_n^0) \sin(2\pi n/N)}{\sum_n (r_n(t) - r_n^0) \cos(2\pi n/N)}$$

in which r^0 is the dimerized lattice displacement of the pristine chain without defects.

From Figures 1 and 2, one can also find that, after the external electric field is smoothly turned on, the polaron is accelerated at first and then moves with a nearly constant velocity as one entity consisting of both the charge and the lattice deformation. We calculate the positions of the center of a polaron during the transport process according to eq 6 and show the temporal evolution of the polaron center position in Figure 3. It can be clearly seen that the center position of the polaron increases nearly linearly with the increase of time after the initial short-time acceleration. This implies that the polaron defect is transported with a nearly constant velocity and supports our

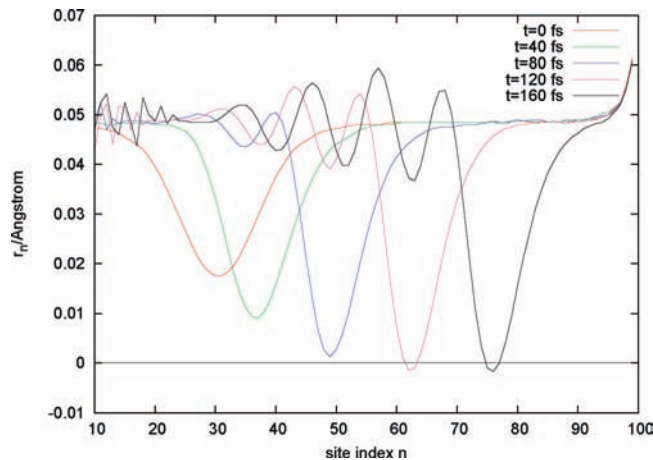


Figure 2. Time evolution of the staggered bond order parameter r_n in a polymer chain with the transport of a polaron under an external electric field (the polaron moves from the left to the right) ($E_0 = 3.0$ mV/Å, $U = 2.0$ eV, $V = 1.0$ eV).

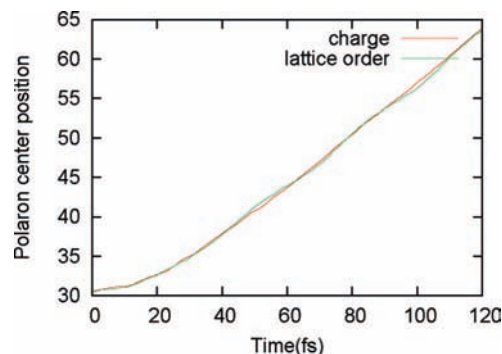


Figure 3. Temporal evolution of the center position of a polaron under an external electric field derived from both the charge density and the bond order parameter ($E_0 = 3.0$ mV/Å, $U = 2.0$ eV, $V = 1.0$ eV).

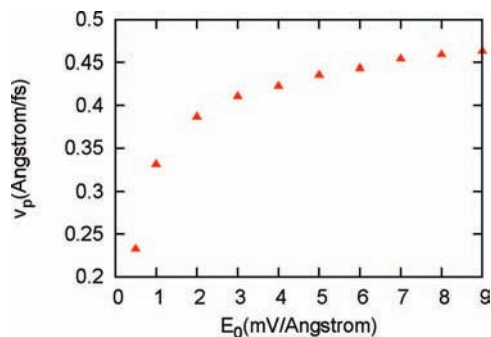


Figure 4. The stationary velocity of a polaron v_p as a function of the electric field strength ($U = 2.0$ eV, $V = 1.0$ eV).

observation from Figures 1 and 2. Therefore, only the stationary velocity will be considered for polaron transport in the following discussions. Meanwhile, one also finds that the lattice distortion center always stays well together with the charge density center. However, it should also be noticed that, under high electric field strength, the deviation of the lattice distortion center position from the charge density center position may become much larger because the charge density moves much faster under high field and the lattice distortion cannot catch up with the charge density. This separation between the charge center and lattice distortion center may lead to the dissociation of a polaron. The dissociation of a polaron under high electric field strength will be discussed in the next section.

B. Relationship between Polaron-Transport Velocity and Electric Field Strength. The dependence of the stationary velocity of a polaron v_p on the electric field strength is shown in Figure 4. We find that v_p increases with increasing electric field strength. Apparently, the polaron velocity can easily exceed the sound speed ($V_s = (4K/M)^{1/2}a/2 = 0.15$ Å/fs), and the maximum velocity (about $3 V_s$) is reached at a high electric field strength (~ 9 mV/Å). Moreover, a very interesting behavior of v_p as a function of the electric field strength is observed. An ohmic region where v_p increases nearly linearly with the electric field strength is found. This ohmic region extends approximately from 3 to 9 mV/Å for the case of $U = 2.0$ eV and $V = 1.0$ eV. Below 3 mV/Å, the polaron velocity increases nonlinearly, and when $E_0 \geq 10$ mV/Å, the polaron becomes unstable, and the charge will be decoupled from the lattice distortion.

We illustrate the temporal evolutions of the polaron center position under different external electric field strengths in Figure 5. We can find that the lattice distortion center stays well together with the charge center under low electric field strengths. However, the deviation of the lattice distortion center from the charge density center becomes much larger under higher electric field strengths because the charge density moves much faster under high field and the lattice distortion cannot catch up with the charge density. Under the electric field of 10 mV/Å, the distance between the two centers becomes even larger than several unit distances, implying that the polaron has been completely dissociated. This dissociation can be clearly seen from the time evolution pictures of charge density and the staggered bond order parameter in a polymer chain with a polaron defect under an external electric field of 10 mV/Å in Figures 6 and 7. While the charge density accelerates to a high speed as shown in Figure 6, the original lattice distortion stays far behind the charge density with a distance of more than tens of unit distances. The charge density will induce new lattice distortion in the nearby region around the charge density center, while the original lattice distortion can hardly move further, as illustrated in Figure 7. Therefore, the polaron defect has become

completely dissociated under the high electric field. One issue we should mention is that there might be boundary effects on the polaron dissociation at high electric fields in our calculations because our model chain is not very long (it contains only 100 monomers). As can be found in Figure 5, both the lattice distortion center and the charge center move back and forth after about 65 fs after the turn-on of a high electric field of $E_0 = 10.0$ mV/Å. Obviously, the backward motion of the polaron center is caused by the reflection by the chain boundary. However, we notice that the distance between has been very large before 60 fs after the turn-on of such a high electric field, which implies that the polaron has become dissociated before the polaron center gets near the chain end. Therefore, we consider that our model chain is long enough to study the polaron dissociation phenomenon, and an increase of the model chain length will not change the calculated threshold field strength for polaron dissociation.

Apparently, our calculated threshold field strength of around 10 mV/Å for polaron dissociation is in agreement with the value of 9.5 mV/Å obtained by SSH-EHM/UHF calculations by Di et al.²³ and much closer to the experimentally determined value of about 15 mV/Å⁵² compared to the value of 6 mV/Å calculated by Rakhmanova and Conwell^{9,10} and 3.5 mV/Å calculated by Johansson and Stafström.^{13,14} The large deviations of the calculated threshold field strength from the experimental value by the latter two groups are due to the fact that they considered only the SSH model and considered no electron–electron interactions in their studies, and the agreement of SSH-EHM calculations with experimental results shows again that the inclusion of electron–electron interactions is vital for the theoretical studies of charge carriers in conducting polymers. Another thing that should be noticed is that our U (2.0 eV) and V values (1.0 eV) are not the standard values for any special kind of polymers. Here, we use these two values only for the purpose of showing how a polaronic transport will generally evolve and whether the inclusion of electron–electron interactions is important for a reasonable theoretical simulation of the polaronic transport process. The detailed discussion of how the on-site repulsions U and the nearest-neighbor interactions V will influence the polaronic transport will be shown in the next sections.

C. Influence of On-Site Repulsions U on Polaron-Transport Velocity. In order to study the influence of electron–electron interactions on polaron transport, we focus on the stationary velocity of a polaron v_p calculated with different electron–electron interaction strengths under the constraint that the other parameters are fixed. It should be noticed that the real conjugated polymer is with weak interactions. Strong interactions will lead to too strong charge polarizations, which are unrealistic. Considering that we are only focusing on the study of a real conjugated polymer system, in this work, we adopt only the weak-interaction parameters ($U < 2t, V < t$).

First, we study the Hubbard model with only on-site Coulomb interactions U , that is, $V = 0$ in the EHM. The dependence of the polaron stationary velocity v_p on the on-site Coulomb interactions U is displayed in Figure 8. We find that v_p decreases monotonically with the increasing U value, and its maximum value is achieved at $U = 0.0$ eV. This can be easily understood because the variation of the charge carrier transport velocity is strongly related to the delocalization level of the charge carrier defect. The lattice tends to be occupied by one electron per site when the on-site Coulomb repulsion U increases. Therefore, an increasing U will lead to more localized charge density and

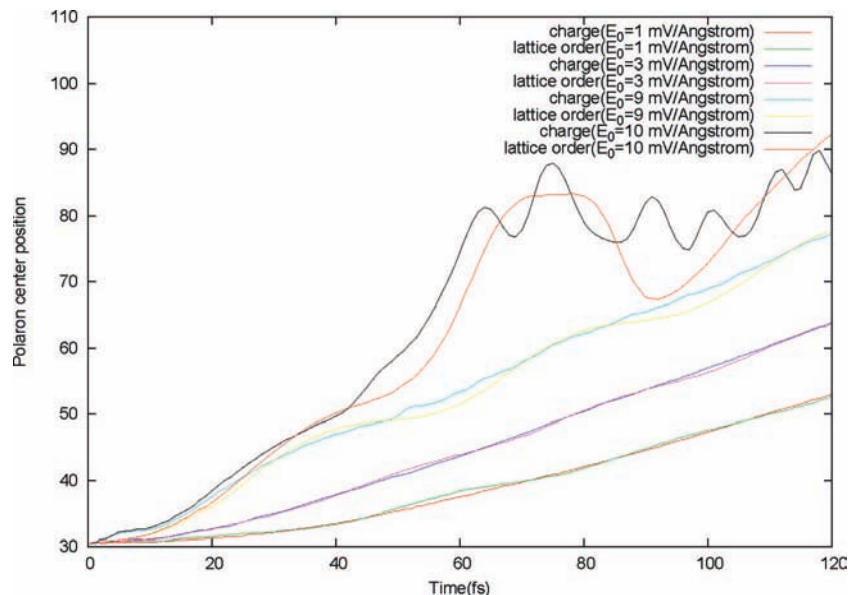


Figure 5. Temporal evolution of the center position of a polaron under different external electric field strengths ($U = 2.0$ eV, $V = 1.0$ eV).

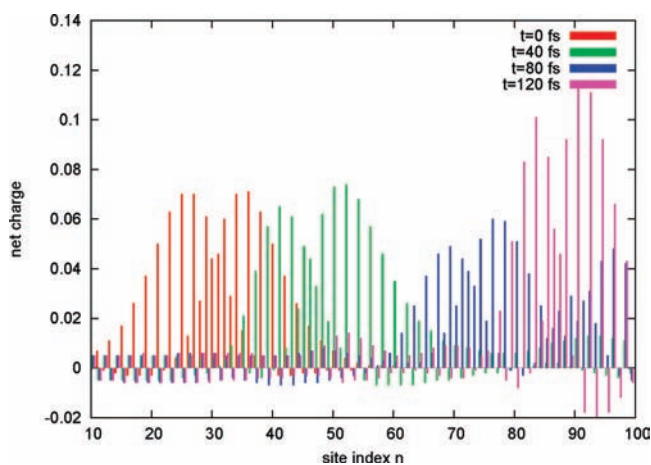


Figure 6. Time evolution of net charge distribution in a polymer chain with the transport of a polaron under a high external electric field (the polaron moves from the left to the right) ($E_0 = 10.0$ mV/Å, $U = 2.0$ eV, $V = 1.0$ eV).

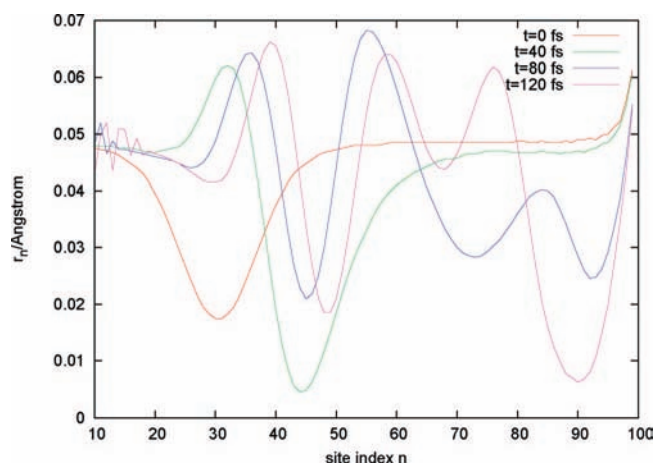


Figure 7. Time evolution of the staggered bond order parameter r_n in a polymer chain with the transport of a polaron under a high external electric field (the polaron moves from the left to the right) ($E_0 = 10.0$ mV/Å, $U = 2.0$ eV, $V = 1.0$ eV).

a smaller defect width of the polaron and accordingly restrain the polaron transport. This analysis is supported by our calculated charge density width values of a static polaron W_c . W_c is calculated according to the following formula

$$W_c = \left(\sum_n [n - X_c]^2 \rho_n \right)^{1/2} \quad (8)$$

Through calculations, we find the polaron width W_c also decreases monotonically with an increasing U value, from 10.10 ($U = 0.0$ eV) to 9.68 ($U = 1.5$ eV) and then to 7.62 ($U = 4.0$ eV). This sequence is in agreement with that of the polaron stationary velocity v_p and supports our analysis of the relationship between the polaron-transport velocity and the delocalization level of a polaron. Actually, the change of the polaron delocalization can also be directly viewed through the geometrical picture of the static polaron defect. In Figure 9, the staggered bond order parameter r_n of a static polaron calculated by different U values is shown. It can be clearly seen that the lattice dimerization is enhanced and that the polaron width becomes narrower while the U value increases. All of these pictures show that the polaron transport is suppressed by the

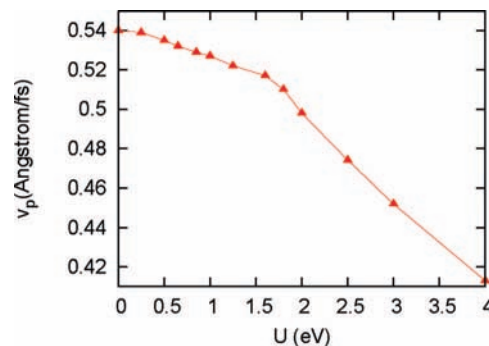


Figure 8. The stationary transport velocity of a polaron as a function of different U values ($E_0 = 3.0$ mV/Å, $V = 0.0$ eV).

on-site Coulomb repulsions U . The monotonic decrease picture of polaron-transport velocity with on-site Coulomb repulsions U observed by us is in agreement with Di et al.'s UHF calculations²³ and Zhao et al.'s recent adaptive TDDMRG results⁵⁰ but not in accordance with our recent studies on charged soliton transport, in which we found that charged-soliton-transport velocity is nonmonotonic in U .⁵¹ The different

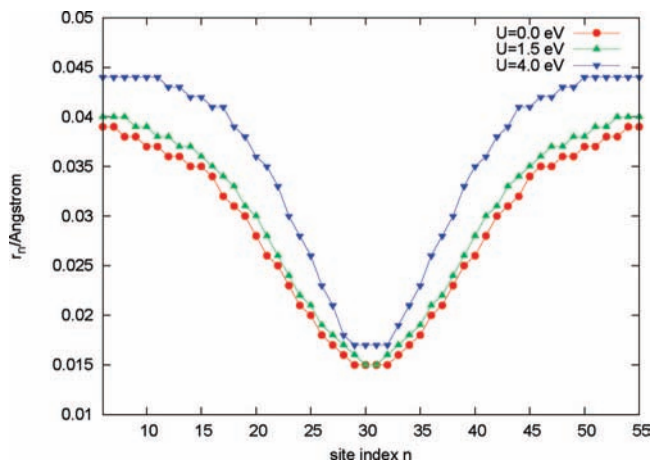


Figure 9. The staggered bond order parameter r_n of a static polaron for several different U values ($V = 0.0$ eV).

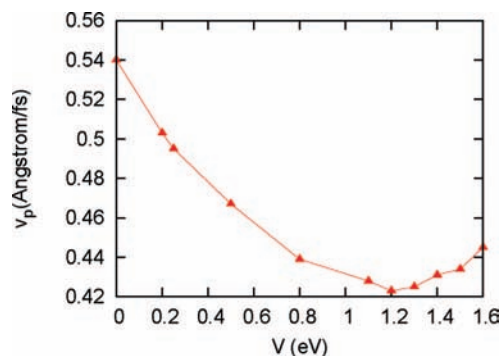


Figure 10. The stationary transport velocity of a polaron as a function of different V values ($E_0 = 3.0$ mV/Å, $U = 0.0$ eV).

behaviors of charge carrier transport with U increasing is due to the different characteristics of charged solitons and polarons. It was found that the polaron defect is more delocalized than the charged soliton defect and that the height of the charge density peaks in polarons is only roughly one-half that of the charge density peaks in charged solitons.³⁹ In a more localized case with large charge densities, as in a charged soliton, a small U may favor the charge carrier transport because the increasing on-site repulsion for large charge densities can make the electron (or hole) hop more easily to the next site. Therefore, the different behaviors of charge carrier transport with U increasing for charged solitons and polarons are reasonable.

D. Influence of Nearest-Neighbor Interactions V on Polaron-Transport Velocity. Second, we also study the influence of nearest-neighbor electron–electron interactions V on the polaron-transport process. The dependence of the stationary velocity of a polaron v_p on the V values is displayed in Figure 10, where U values are supposed to be frozen to be zero. This assumption is not realistic because the on-site Coulomb interactions U are normally much stronger than the neighbor electron–electron interactions V ; we make this assumption only for the purpose of studying of the influence of V on the polaron transport process without the effect of U . As can be seen in Figure 10, the situation is completely different from the case of an on-site Coulomb interaction. Interestingly, v_p is non-monotonic in V ; it decreases to a shallow minimum at $V \approx 1.2$ eV gradually and then increases again. In fact, similar to the case discussed above with varying U , the variation of v_p with V is also strongly related to changing the delocalization of the polaron defect. For small V , larger positive charge densities will be induced in the central part of a polaron defect while the

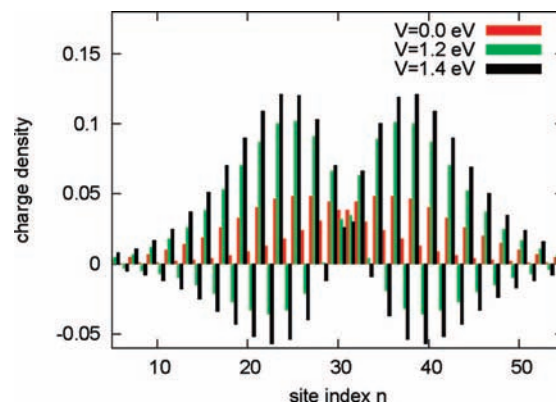


Figure 11. The charge density of a static polaron as a function of the site index calculated with different V values ($U = 0.0$ eV).

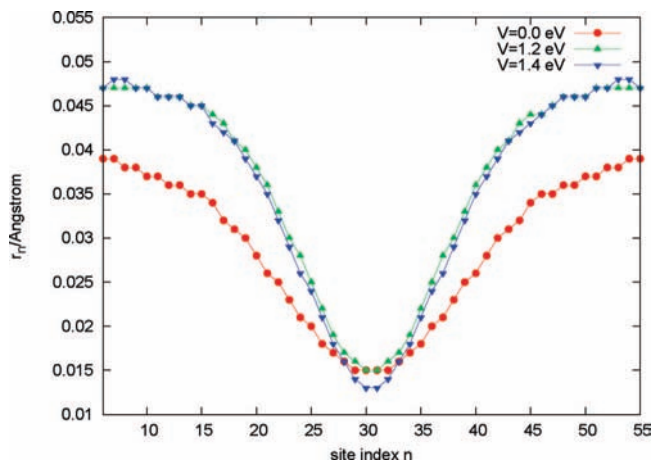


Figure 12. The staggered bond order parameter r_n of a static polaron for several different V values ($U = 0.0$ eV).

induced negative charge densities at nearest-neighbor sites are still relatively small, as shown in Figure 11. Therefore, the polaron defect tends to be more localized, and consequently, the polaron transport becomes more difficult. So, v_p decreases while the value of V increases from 0.0 to 1.2 eV, as displayed in Figure 10. However, when nearest-neighbor electron–electron interactions V increase further and become dominant, very large charge polarization will be induced. Therefore, the electron–hole attraction between opposite charge densities at nearest-neighbor sites will contribute much more significantly to the polaron system and favor the hoppings of the accumulated electrons (or holes) in the central part of a polaron defect to the neighbor sites. As shown in Figure 11, the two positive charge density peaks are separated further when V increases from 1.2 to 1.4 eV. This change leads to a more delocalized polaron defect and accordingly the increase of v_p . Our calculated polaron charge density width results, namely, that W_c decreases gradually from 10.10 ($V = 0.0$ eV) to 9.37 ($V = 1.2$ eV) and then increase gradually to 9.89 ($V = 1.4$ eV), support our analysis well. In order to directly view the change of the delocalization level of the polaron defect through geometrical pictures, we also show the staggered bond order parameter r_n of a static polaron calculated with different V values in Figure 12. It is clearly shown that the lattice dimerization is enhanced and that the polaron width becomes narrower with V for small V . We also find that the polaron becomes more delocalized with a smaller r_n minimum while V increases further from 1.2 to 1.4 eV. The change of polaron delocalization illustrated from the geometrical picture is in accordance with what has been shown in the charge density picture, verifying that small V suppresses the polaronic

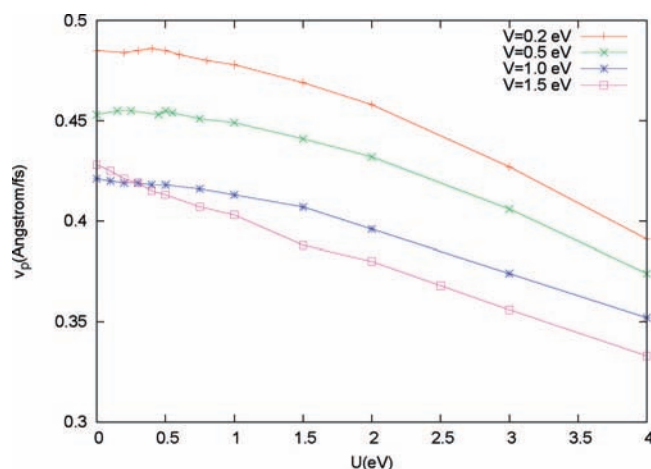


Figure 13. The stationary transport velocity of a polaron as a function of U for fixed values of V ($E_0 = 3.0$ mV/Å).

transport while large V favors the polaron transport. This nonmonotonic picture of polaron-transport velocity in V is similar to that observed in charged soliton transport.⁵¹

E. Influence of Both the On-Site Coulomb Interactions U and the Nearest-Neighbor Interactions V on Polaron-Transport Velocity. Furthermore, we consider the realistic case of conducting polymers in which both the on-site Coulomb interactions U and the nearest-neighbor interactions V are taken into account. Figure 13 shows the stationary transport velocity of a polaron v_p as a function of U for fixed values of $V = 0.2, 0.5, 1.0,$ and 1.5 eV. Generally, the v_p behavior with varied U and fixed V values is quite similar to that illustrated in Figure 8 in which V is frozen to be 0.0 eV. It can be found that v_p decreases monotonically with U . Meanwhile, we can also find that v_p seems to decrease more rapidly in large V cases than in small V cases for small U . Larger nearest-neighbor electron–electron interactions V will lead to larger charge polarizations, and of course, the increasing on-site Coulomb repulsions U will suppress the transport of a polaron associated with larger charge polarizations more significantly compared to the case with smaller charge polarizations. Therefore, the suppression of polaron transport by the on-site Coulomb repulsions U is more remarkable in large V cases than that in small V cases. The monotonic decrease picture of polaron-transport velocity with on-site Coulomb repulsions U observed by us is opposed to the nonmonotonic picture obtained by Di et al. through UHF calculations.²³ They found that a local extremum of the stationary velocity of the polaron can be achieved at $U \approx 2V$. The difference between the results of the adaptive TDDMRG and UHF calculations is due to the fact that the latter method ignores the important electron correlation effect. Previous theoretical static studies have found that neglecting electron correlation effects will lead to an underestimation of the defect width as well as an overestimation of charge polarization.^{34–37} In a more localized case with large charge densities, presented by UHF calculations without the inclusion of electron correlation effect, introducing a small U may favor the charge carrier transport because the increasing on-site repulsion for large charge densities can make the electron (or hole) hop more easily to the next site. Therefore, the difference between TDDMRG and UHF calculations shows again that the electron correlation effect plays an important role in describing the charge carrier properties.

IV. Summary and Conclusion

For a model conjugated polymer chain initially holding a polaron defect, described using the combined SSH-EHM model extended with an additional part for the influence of an external electric field, we have studied the dynamics of polaron transport through this chain by virtue of simulating the backbone monomer displacements with classical MD and evolving the wave function for the π electrons with the adaptive TDDMRG.

It is found that after a smooth turn-on of the external electric field, the polaron is accelerated at first up to a stationary constant velocity as one entity consisting of both the charge and the lattice deformation. During the entire time evolution process, the geometrical distortion curve and charge distribution shape for the polaron defect always stay well coupled and show no dispersion under low external electric fields, implying that the polaron defect is an inherent feature and the fundamental charge carrier in conducting polymers. The dependence of the stationary velocity of a polaron v_p on the external electric field strength is also studied, and an ohmic region where v_p increases linearly with the field strength is found. Values beyond the speed of sound are achievable. This ohmic region extends approximately from 3 to 9 mV/Å for the case of $U = 2.0$ eV and $V = 1.0$ eV. Below 3 mV/Å, the polaron velocity increases nonlinearly, and in high external electric field strengths, the polaron will become unstable and dissociate. Our calculated threshold field strength for polaron dissociation is around 10 mV/Å for the case of $U = 2.0$ eV and $V = 1.0$ eV. It is in good agreement with experimental results and more physically intuitive than previous SSH calculations, which take no electron–electron interactions into account.

The influence of electron–electron interactions (both the on-site Coulomb interactions U and the nearest-neighbor interactions V) on polaron transport are investigated in detail. In general, the increase of the on-site Coulomb interactions U makes the lattice tend to be occupied by one electron per site and accordingly suppress the polaron transport. Therefore, v_p decreases monotonically with U . Meanwhile, small V values are not beneficial to the polaronic motion because they induce a more localized defect distribution, and due to the induced large charge polarization accompanied with large nearest-neighbor attractions, large V values favor the polaron transport. When U and V are considered at the same time, v_p also decreases monotonically with the increasing U value, and v_p decreases more rapidly for small U in large V cases than in small V cases.

Acknowledgment. H.M. is grateful to Andrej Gendiar for helpful discussions. H.M. also acknowledges the support by an Alexander von Humboldt Research Fellowship.

References and Notes

- (1) Chiang, C. K.; Fincher, C. R.; Park, Y. W.; Heeger, A. J.; Shirakawa, H.; Louis, E. J.; Gau, S. C.; MacDiarmid, A. G. *Phys. Rev. Lett.* **1977**, *39*, 1098.
- (2) Shirakawa, H.; Louis, E. J.; MacDiarmid, A. G.; Chiang, C. K.; Heeger, A. J. *J. Chem. Soc., Chem. Commun.* **1977**, *16*, 579.
- (3) Chiang, C. K.; Drury, M. A.; Gau, S. C.; Heeger, A. J.; Louis, E. J.; MacDiarmid, A. G.; Park, Y. W.; Shirakawa, H. *J. Am. Chem. Soc.* **1978**, *100*, 1013.
- (4) MacDiarmid, A. G. *Synth. Met.* **1997**, *84*, 27.
- (5) Burroughes, J. H.; Jones, C. A.; Friend, R. H. *Nature* **1998**, *335*, 137.
- (6) Heeger, A. J. *J. Phys. Chem. B* **2001**, *105*, 18475.
- (7) Heeger, A. J. *Rev. Mod. Phys.* **2001**, *73*, 681.
- (8) Heeger, A. J.; Kivelson, S.; Schrieffer, J. R.; Su, W. P. *Rev. Mod. Phys.* **1988**, *60*, 781.
- (9) Rakhmanova, S. V.; Conwell, E. M. *Appl. Phys. Lett.* **1999**, *75*, 1518.
- (10) Rakhmanova, S. V.; Conwell, E. M. *Synth. Met.* **2000**, *110*, 37.

- (11) Basko, D. M.; Conwell, E. M. *Phys. Rev. Lett.* **2002**, *88*, 056401.
(12) Arikabe, Y.; Kuwabara, M.; Ono, Y. *J. Phys. Soc. Jpn.* **1996**, *65*, 1317.
(13) Johansson, Å; Stafström, S. *Phys. Rev. Lett.* **2001**, *86*, 3602.
(14) Johansson, Å; Stafström, S. *Phys. Rev. Lett.* **2004**, *69*, 235205.
(15) Streitwolf, H. W. *Phys. Rev. B* **1998**, *58*, 14356.
(16) Yan, Y. H.; An, Z.; Wu, C. Q. *Eur. Phys. J. B* **2004**, *42*, 157.
(17) Yu, J. F.; Wu, C. Q.; Sun, X.; Nasu, K. *Phys. Rev. B* **2004**, *70*, 064303.
(18) Fu, J.; Ren, J.; Liu, X.; Liu, D.; Xie, S. *Phys. Rev. B* **2006**, *73*, 195401.
(19) Liu, X.; Gao, K.; Fu, J.; Li, Y.; Wei, J.; Xie, S. *Phys. Rev. B* **2006**, *74*, 172301.
(20) Li, Y.; Liu, X.; Fu, J.; Liu, D.; Xie, S.; Mei, L. *Phys. Rev. B* **2006**, *74*, 184303.
(21) Su, W. P.; Schrieffer, J. R.; Heeger, A. J. *Phys. Rev. Lett.* **1979**, *42*, 1698.
(22) Su, W. P.; Schrieffer, J. R.; Heeger, A. J. *Phys. Rev. B* **1980**, *22*, 2099.
(23) Di, B.; An, Z.; Li, Y. C.; Wu, C. Q. *Europhys. Lett.* **2007**, *79*, 17002.
(24) Yonemitsu, K.; Ono, Y.; Wada, Y. *J. Phys. Soc. Jpn.* **1988**, *57*, 3875.
(25) Sim, F.; Salahub, D. R.; Chin, S.; Dupuis, M. *J. Chem. Phys.* **1991**, *95*, 4317.
(26) Suhai, S. *Int. J. Quantum Chem.* **1992**, *42*, 193.
(27) Villar, H. O.; Dupuis, M. *Theor. Chim. Acta* **1992**, *83*, 155.
(28) Bally, T.; Roth, K.; Tang, W.; Schrock, R. R.; Knoll, K.; Park, L. Y. *J. Am. Chem. Soc.* **1992**, *114*, 2440.
(29) Rodríguez-Monge, L.; Larsson, S. *J. Chem. Phys.* **1995**, *102*, 7106.
(30) Hirata, S.; Torii, H.; Tasumi, M. *J. Chem. Phys.* **1995**, *103*, 8964.
(31) Fülischer, M. P.; Matzinger, S.; Bally, T. *Chem. Phys. Lett.* **1995**, *236*, 167.
(32) Guo, H.; Paldus, J. *Int. J. Quantum Chem.* **1997**, *63*, 345.
(33) Perpète, E. A.; Champagne, B. *J. Mol. Struct.: THEOCHEM* **1999**, *487*, 39.
(34) Fonseca, T. L.; Castro, M. A.; Cunha, C.; Amaral, O. A. V. *Synth. Met.* **2001**, *123*, 11.
(35) Oliveira, L. N.; Amaral, O. A. V.; Castro, M. A.; Fonseca, T. L. *Chem. Phys.* **2003**, *289*, 221.
(36) Champagne, B.; Spassova, M. *Phys. Chem. Chem. Phys.* **2004**, *6*, 3167.
(37) Monev, V.; Spassova, M.; Champagne, B. *Int. J. Quantum Chem.* **2005**, *104*, 354.
(38) Ma, H.; Cai, F.; Liu, C.; Jiang, Y. *J. Chem. Phys.* **2005**, *122*, 104909.
(39) Ma, H.; Liu, C.; Jiang, Y. *J. Phys. Chem. B* **2006**, *110*, 26488.
(40) Hu, W.; Ma, H.; Liu, C.; Jiang, Y. *J. Chem. Phys.* **2007**, *126*, 044903.
(41) White, S. R. *Phys. Rev. Lett.* **1992**, *69*, 2863.
(42) White, S. R. *Phys. Rev. B* **1993**, *48*, 10345.
(43) Schollwöck, U. *Rev. Mod. Phys.* **2005**, *77*, 259.
(44) White, S. R.; Feiguin, A. *Phys. Rev. Lett.* **2004**, *93*, 076401.
(45) Daley, A. J.; Kollath, C.; Schollwöck, U.; Vidal, G. *J. Stat. Mech.* **2004**, P04005.
(46) Gobert, D.; Kollath, C.; Schollwöck, U.; Schütz, G. *Phys. Rev. E* **2005**, *71*, 036102.
(47) Kollath, C.; Schollwöck, U.; Zwerger, W. *Phys. Rev. Lett.* **2005**, *95*, 176401.
(48) Kleine, A.; Kollath, C.; McCulloch, I. P.; Giamarchi, T.; Schollwöck, U. *Phys. Rev. A* **2008**, *77*, 013607.
(49) Cramer, M.; Flesch, A.; McCulloch, I. P.; Schollwöck, U.; Eisert, J. *Phys. Rev. Lett.* **2008**, *101*, 063001.
(50) Zhao, H.; Yao, Y.; An, Z.; Wu, C. Q. *Phys. Rev. B* **2008**, *78*, 035209.
(51) Ma, H.; Schollwöck, U. *J. Chem. Phys.* **2008**, *129*, 244705.
(52) Lin, H. N.; Lin, H. L.; Wang, S. S.; Yu, L. S.; Perng, G. Y.; Chen, S. A.; Chen, S. H. *Appl. Phys. Lett.* **2002**, *81*, 2572.

JP809045R